Hindawi Publishing Corporation
Mathematical Problems in Engineering
Volume 2015, Article ID 321085, 10 pages
http://dx.doi.org/10.1155/2015/321085

Research Article

Structure Optimization Design of the Electronically Controlled Fuel Control Rod System in a Diesel Engine

Hui Jin and Haosen Wang

School of Mechanical Engineering, Beijing Institute of Technology, Beijing 100081, China

Correspondence should be addressed to Hui Jin; jinhui@bit.edu.cn

Received 30 July 2014; Accepted 24 October 2014

Academic Editor: Hong Chen

Poor ride comfort and shorter clutch life span are the key factors restricting the commercialization of automated manual transmission (AMT). For nonelectrically controlled engines or AMT where cooperative control between the engine and the transmission is not realizable, applying electronically controlled fuel control rod systems (ECFCRS) is an effective way to solve these problems. By applying design software such as CATIA, Matlab and Simulink, and MSC Adams, a suite of optimization design methods for ECFCRS drive mechanisms are developed here. Based on these new methods, design requirements can be analyzed comprehensively and the design scheme can be modified easily, thus greatly shortening the design cycle. The bench tests and real vehicle tests indicate that the system developed achieves preferable engine speed following-up performance and engine speed regulating performance. The method developed has significance as a reference for developing other vehicle systems.

1. Introduction

Based on manual transmission, automated manual transmission, or AMT in short, realizes clutch operation and gear shifting by using electrohydraulic [1, 2], electromechanical [3–5], or electropneumatic [6] actuators instead of the driver's direct manipulation of the clutch and shift handle. Thanks to its simple structure, low cost, and high transmission efficiency, the application of AMT to vehicles has been continually increasing. AMT has now been applied in several car models, such as the Volkswagen Lupo, Honda Civic, BWM M3, Benz Smart, and others [7–9].

Poor ride comfort and shorter clutch life span are the key factors restricting the commercialization of AMT [10, 11], and many different methods of clutch engagement control [12–15] and engine throttle control [2, 16–19] have been proposed to address these issues. For nonelectrically controlled diesel engines or AMT systems in which cooperative control between the diesel engine and the transmission is not realizable, however, applying an electronically controlled fuel control rod system (ECFCRS) is an effective way to solve these problems.

Optimizing the design of the drive mechanism is the key to realizing ECFCRS. Only with a drive mechanism possessing a simple structure, reliable performance characteristics, and convenient maintenance can ECFCRS with preferable performance be achieved. This paper develops a suite of optimization design method for the drive mechanism of an ECFCRS, using such assistant design softwares as CATIA, Matlab and Simulink, and MSC Adams, and covering the design principles and design methods of the drive mechanism, design schemes comparison, the design philosophy of all parts of the mechanism, the structural design and strength checking of the mechanism's parts, the assembly design of the drive mechanism, and bench tests, and real vehicle tests of the developed system.

2. Design Principles and Design Method

During drive mechanism design, the following aspects should be considered: ① that the developed electric motor drive mechanism can be installed onto the engine with ease and the whole system can operate steadily; ② that no dead

points or turning points can exist during the working range; ③ that the developed mechanism guarantees as much as possible a preferable linear relationship between the rotation angle of the motor output arm and that of fuel control rod (otherwise the system may be instable); ④ that the parts of which the mechanism consists should be as simple as possible, ideally standard, or interchangeable parts, in order to decrease processing costs and facilitate easy assembly and maintenance.

2.1. Design Method of the Drive Mechanism. Based on design softwares as CATIA, Matlab and Simulink, and MSC Adams, a design flow is developed to increase the efficiency of research, development, design, testing and evaluation of the system. The design requirements can thus be analyzed comprehensively and the design schemes can be modified rapidly, greatly shortening the design cycle.

The developed design flow is as follows.

(1) Mathematical analysis: carry out qualitative and preliminary quantitative analysis of the investigated system utilizing the theories and formulae of classical mechanics to orient the research and design. This step is accomplished with the Matlab development environment.

(2) 3D model establishment: establish a 3D model of the developed mechanism through CATIA based on the parts' geometric designs and the mechanism assembly designs. This facilitates easy analysis of the spatial arrangement of the mechanism.

(3) Kinematics and kinetic analysis: carry out analysis of kinematics and kinetic characteristics of the mechanism model created in CATIA using Adams. If the mechanism cannot meet the requirements in terms of kinematics and kinetic characteristics, return to CATIA and modify the geometric parameters of the parts.

(4) Analysis of control performance: analyze the control performance of the mechanism with Adams and Simulink to supply reference for developing the control software.

(5) Processing of parts: perform strength checking of the parts, generate the 2D drawings from CATIA, and complete parts processing.

(6) System performance tests: verify whether the ECFCRS with the mechanism developed has preferable engine speed following-up and regulating performances based on bench tests and real vehicle tests.

2.2. Design Schemes Comparison. To realize the control of the electric motor on the fuel control rod of a diesel engine, three schemes are considered: ① directly driving the fuel control rod by an electric motor; ② driving the fuel control rod through a chain and turntable driven by an electric motor; ③ driving the fuel control rod by an electric motor via rod linkage mechanisms.

Scheme 1 is the simplest in the mechanical structure, with the rotation angle of the electric motor's output arm and that of the fuel control rod being completely synchronized, but the positional tolerance zone of the electric motor's bracket and the installation site of the electric motor require extreme precision. Scheme 2 has the best force moment magnification characteristics, so that an electric motor with smaller output torque can be used, and the spatial arrangement of the mechanism is relatively flexible and less restricted due to the flexible driving link. The mechanism structure is however more complicated, and the parts utilized are generally not standard or interchangeable, which is disadvantageous to processing and maintenance. Scheme 3 has the relatively simple structure and the requirements in terms of design accuracy are not high. Also, the standard and interchangeable parts may be easily used and processing and maintenance are convenient. This scheme can gain certain force moment magnification characteristics through optimizing the parts' parameters so that an electric motor with smaller output torque can be used. Its disadvantages lie in that a turning point or dead point may exist in the system. If this scheme is adopted, the system should therefore be optimized during design to solve these potential problems.

Based on comprehensive evaluation, scheme 3 was selected, namely, driving the fuel control rod via a rod linkage mechanism. Although this scheme does not achieve the optimal kinematics characteristics or force moment magnification characteristics, it can balance these two factors well and has preferable performance in terms of processing and maintenance characteristics.

3. Design Philosophy of the Drive Mechanism's Parts

3.1. Determination of Fuel Control Rod Length and Electric Motor's Output Arm Length

3.1.1. Determination of Fuel Control Rod Length. The length of the fuel control rod was designed as 40 mm, after consideration of the spatial arrangement of the engine and the use of this value as a base to optimize the parameters of other parts of the mechanism.

3.1.2. Determination of Electric Motor's Output Arm Length. The length of the electric motor's output arm can influence whether the output force moment thereof is magnified or reduced and can also influence the slewing area of the electric motor's output arm. This length may be determined according to the following calculation.

In Figure 1, O_0, the grid origin of Reference Frame $\mathbf{O}_0$, and O_1, the grid origin of Reference Frame $\mathbf{O}_1$, are the cooperation centers of the fuel control rod and fuel control shaft and of the electric motor's output arm and electric motor's rotary shaft, respectively, and the $\mathbf{x}_0$ axis and $\mathbf{x}_1$ axis refer to the fuel control shaft and motor shaft, respectively, with their respective vectors being $\mathbf{U}_0$ and $\mathbf{U}_1$. The two connection joints (ball pivots) of the link rod of the mechanism are within Surface $\mathbf{y}_0\mathbf{z}_0$ and Surface $\mathbf{y}_1\mathbf{z}_1$, respectively.

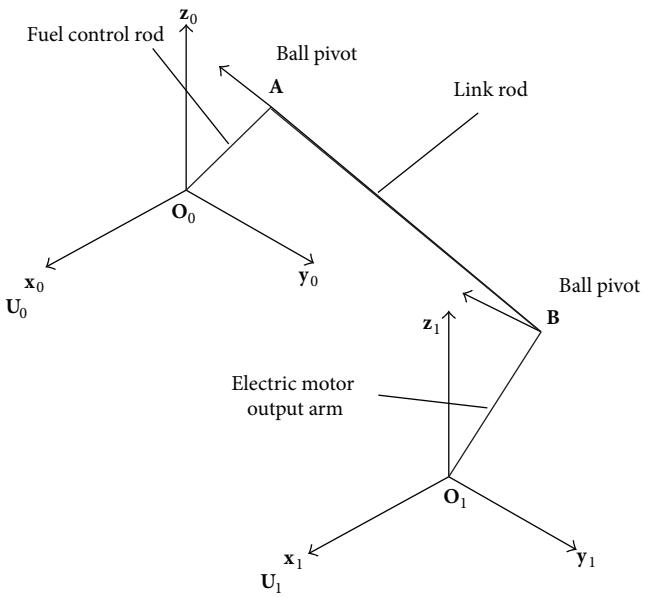

Figure 1: Schematic diagram of the rod linkage mechanism of the ECFCRS.

Definition:

$$\begin{aligned}
\mathbf{O}_0 &= \left[X_0, Y_0, Z_0\right]^{\mathbf{T}},\\
\mathbf{O}_1 &= \left[X_1, Y_1, Z_1\right]^{\mathbf{T}},\\
\mathbf{A} &= \left[X_A, Y_A, Z_A\right]^{\mathbf{T}},\\
\mathbf{A}_0 &= \left[X_A^0, Y_A^0, Z_A^0\right]^{\mathbf{T}},\\
\mathbf{B} &= \left[X_B, Y_B, Z_B\right]^{\mathbf{T}},\\
\mathbf{B}_0 &= \left[X_B^0, Y_B^0, Z_B^0\right]^{\mathbf{T}},\\
\mathbf{U}_0 &= \left[X_{U_0}, Y_{U_0}, Z_{U_0}\right]^{\mathbf{T}},\\
\mathbf{U}_1 &= \left[X_{U_1}, Y_{U_1}, Z_{U_1}\right]^{\mathbf{T}}.
\end{aligned} \tag{1}$$

Reference Frame $\mathbf{O}_0$ is selected as the reference frame; therefore

$$\begin{aligned}
\mathbf{O}_0 &= [0, 0, 0]^{\mathbf{T}},\\
\mathbf{U}_0 &= [1, 0, 0]^{\mathbf{T}}.
\end{aligned} \tag{2}$$

In the above definition $\mathbf{A}$ is the coordinate of the ball pivots on the fuel control rod within Reference Frame $\mathbf{O}_0$, $\mathbf{A}_0$ is the initial position of $\mathbf{A}$, $\mathbf{B}$ is the coordinate of the ball pivots on the electric motor's output arm within Reference Frame $\mathbf{O}_1$, $\mathbf{B}_0$ is the initial position of $\mathbf{B}$, $\mathbf{U}_0$ is the vector of fuel control shaft within Reference Frame $\mathbf{O}_0$, $\mathbf{U}_1$ is the vector of the motor shaft within Reference Frame $\mathbf{O}_1$, $\mathbf{O}_1$ is the translation vector of the grid origin of Reference Frame $\mathbf{O}_1$ on Reference Frame $\mathbf{O}_0$, $\mathbf{O}_0\mathbf{A}$ is the effective length of the fuel control rod, $\mathbf{O}_1\mathbf{B}$ is the effective length of the electric motor's output arm, and $\mathbf{AB}$ is the effective length of the link rod.

The length of the electric motor's output arm can be calculated by the following steps.

Step 1. Translate Reference Frame $\mathbf{O}_1$ onto Reference Frame $\mathbf{O}_0$ and match their grid origins together.

Step 2. Rotate Point B to its target location with rotation matrix $\mathbf{Q}_1$.

Step 3. Translate Reference Frame $\mathbf{O}_1$ to its true position:

$$[\mathbf{B}] = [\mathbf{Q}_1]([\mathbf{B}_0] - [\mathbf{O}_1]) + [\mathbf{O}_1], \tag{3}$$

where rotation matrix $\mathbf{Q}_1$ is determined by

$$[\mathbf{Q}_1] = \begin{bmatrix}
2\left(q_0^2 + q_1^2\right) - 1 & 2\left(q_1q_2 - q_0q_3\right) & 2\left(q_1q_3 + q_0q_2\right)\\
2\left(q_1q_2 + q_0q_3\right) & 2\left(q_0^2 + q_2^2\right) - 1 & 2\left(q_2q_3 + q_0q_1\right)\\
2\left(q_1q_3 - q_0q_2\right) & 2\left(q_2q_3 + q_0q_1\right) & 2\left(q_0^2 + q_3^2\right) - 1
\end{bmatrix}. \tag{4}$$

In the above equation, q_0, q_1, q_2, q_3 can be described as

$$\begin{aligned}
q_0 &= \cos\left(\frac{\alpha_1}{2}\right),\\
q_1 &= X_U \sin\left(\frac{\alpha_1}{2}\right),\\
q_2 &= Y_U \sin\left(\frac{\alpha_1}{2}\right),\\
q_3 &= Z_U \sin\left(\frac{\alpha_1}{2}\right),
\end{aligned} \tag{5}$$

where α_1 is the rotation angle from the initial point.

Step 4. Rotate Point A by rotation matrix $\mathbf{Q}_2$ and obtain the coordinates of Point A via numerical methods, to satisfy that Distance $\mathbf{AB}$ equals the intended length of the link rod (namely, the miscalculation is less than the stated upper error limit).

Step 5. With Steps 1 to 4, the calculation of a single point on the mechanism is accomplished, and these steps must be repeated to complete the calculation for the whole slewing area.

Attention must be paid that the rotary shaft vector $\mathbf{U}$, utilized in the rotation matrix, is a unit vector; otherwise the results will be incorrect. The length of the electric motor's output arm can be determined based on these calculations.

3.2. Determination of the Rotation Angle of the Fuel Control Rod and the Electric Motor's Output Arm. The rotation angle of the fuel control rod may be determined according to the requirements of a diesel engine, and rotation within the whole working range should be guaranteed: from the fuel control rod's minimal position to its maximal position. Taking the

EQB235-20 diesel engine of Dongfeng Cummins Engine Co., Ltd. as a sample engine, the rotation angle of the fuel control rod is 45°, and the minimal and maximal positions can be reset by a positive stop bolt. The rotation angle of the electric motor's output arm is thus determined based on the specific design scheme.

The drive mechanism of the ECFCRS should satisfy the following equation:

$$U = W, \tag{6}$$

where U is the work done by the resisting moment of the fuel control rod and W is the work done by the drive torque of the electric motor.

Therefore

$$T_t d\theta_0 = T_m d\theta_1, \tag{7}$$

where T_t is the resistance moment on the fuel control rod, T_m is the electric motor's output torque, θ_0 is the rotation angle of the fuel control rod from the initial position, and θ_1 is the rotation angle of the electric motor's output arm from the initial position.

Differentiating (7) gives

$$T_t \frac{d\theta_0}{dt} = T_m \frac{d\theta_1}{dt}. \tag{8}$$

Namely,

$$T_t \omega_0 = T_m \omega_1, \tag{9}$$

where ω_0 is the angular velocity of the fuel control rod and ω_1 is the angular velocity of the electric motor's output arm.

Equation (7) shows that the larger the rotation angle of the electric motor's output arm, the smaller the average output torque thereof. In terms of the time differential, as in (8), the magnification ratio of the force moment at any point on the mechanism equals the inverse ratio of the two angular velocities. The magnification ratio of the force moment of the mechanism developed will thus be determined by analyzing the ratio of the two angular velocities below.

3.3. Determination of Link Rod Length. The influence of the link rod on the mechanism mainly stems from how it can determine the initial value of the electric motor's rotation angle. In addition, the length of link rod required depends on the installation position of the electric motor.

When the mechanism is of a parallelogrammatic shape, the electric motor's output arm is always parallel to the fuel control rod; namely, $T_m = T_t$, $d\theta_0 = d\theta_1$. In this particular case, the length of the link rod depends only on the installation position of the electric motor.

The curves in Figure 2 represent the drive mechanism's output characteristics when the link rod is 84 mm long and the fuel control rod is 18 mm long. If the angular velocity of the electric motor's output arm is 36°/sec, the simulation period (namely, the horizontal coordinate) is 10 s and the total step number is 500, and then the relevant output characteristics of the fuel control rod can be obtained when

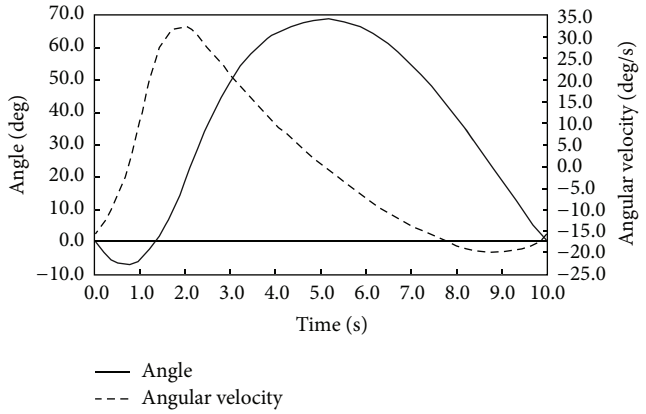

Figure 2: Force moment magnification relationships between fuel control rod and electric motor's output arm.

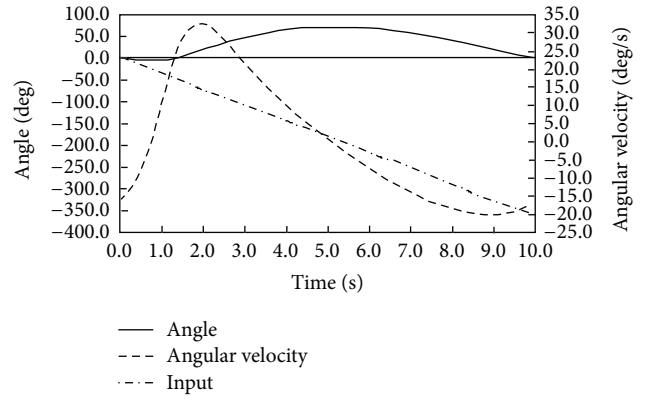

Figure 3: Linearity comparison of fuel control rod and electric motor's output arm.

the electric motor's output arm rotates 360°. Equation (8) indicates that the larger the absolute value of the angular velocity is, the smaller the force moment magnification ratio will be at the corresponding rotation angle. According to Figure 2, the least force moment magnification ratio (absolute value) of the mechanism appears at the peak and the trough of the angular velocity curve.

When analyzing the mechanism, the horizontal coordinate of the curve represents stimulation time, as shown in Figure 2. Because the analysis involves the position characteristics of the mechanism, independent of time, the horizontal coordinate actually refers to the position of the mechanism, namely, the rotation angle of the electric motor's output arm or the rotation angle of the fuel control rod.

Figure 3 is a linearity comparison of the fuel control rod and the electric motor's output arm.

The solid line and the double-dotted chain line in the above figure represent the angle curve of the fuel control rod and the input curve (namely, the angle curve of the electric motor's output arm), respectively. When the two curves' rates of change are equal, the input and output angles of the mechanism are fully linear, and the ratio of these angles can be described by a constant coefficient K. Figure 3 indicates that where the rate of change of the angle of the fuel

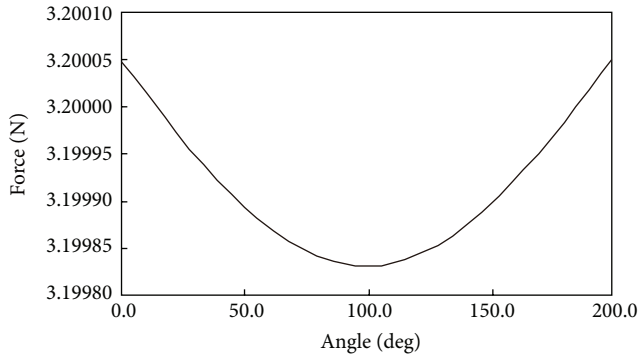

Figure 4: Influence of the included angle between the link rod and the electric motor's output arm on the force of the connection ball pivot.

control rod changes quickly, the linearity of the mechanism decreases, but otherwise the linearity increases. Within 360°, the curve representing the angle of the fuel control rod may be divided into two sections, equidirectional and reversed, with two turning points.

Figures 2 and 3 indicate that the rotation angle of the electric motor's output arm and the initial position of the mechanism can together influence the linear characteristics and magnification characteristics of the mechanism's force moment. Comprehensive consideration is therefore required during selection to ensure said linear characteristics are favorable and to maximize the force moment magnification ratio. During selection of the optimal working interval, the angle and the angular velocity curve can be intercepted by the 120° space interval of the input curve, so that the force moment magnification characteristics and linear characteristics can be compared. A larger rotation angle range for the electric motor's output arm can make control over the mechanism more precise, but the actual design gives priority to the limits of the electric motor's structure and potential processing/installation errors regarding the mechanism's parts.

3.4. Determination of Installation Site of Electric Motor. The installation site of the electric motor is primarily determined by the spatial arrangement of the engine. If this installation site makes the included angles between the link rod with the electric motor's output arm and with the fuel control rod too large or too small, a significant force may be applied to the connection ball pivot.

Figure 4 indicates that when the included angle is 90°, the force (scalar quantity of resultant force) on the ball pivot is at its lowest value and will increase no matter whether the included angle increases or decreases from that point. During design of the mechanism, the included angles of the link rod with the fuel control rod and with the electric motor's output arm should thus be as close to 90° as possible.

3.5. Design of the Retracting Spring. The retracting spring should have two functions: supplying aligning torque to the electric motor, and eliminating any idle clearance formed during the processing and assembly of the drive mechanism's parts.

The ideal retracting spring could supply constant restoring moment (as for a motor shaft) within the whole slewing area. Because a screw extension spring is utilized, such an ideal restoring moment cannot be achieved. The restoring moment that the retracting spring exerts on the electric motor's output arm within the slewing area of the mechanism is nevertheless expected to be as linear as possible.

The free length of the spring should guarantee that the spring is in tension within the whole movement range and that the least restoring moment due to the stretching force can meet the requirements for retraction of the fuel control rod, in order to achieve acceptable performance. Excessive spring stiffness implies that the spring's restoring moment varies dramatically, which is not expected. In light of comprehensive consideration of the free length and aligning torque, a shorter free length and smaller stiffness ratio are relatively ideal for guaranteeing that the mechanism possesses at any position a sufficiently large aligning torque that does not vary too greatly.

The installation site of the electric motor's retracting spring is mostly contingent on the structure of the mechanism and the layout of the motor, in order to guarantee firm installation and reliable operation. No interference exists between the drive mechanism and nearby engine parts.

4. Implementation of the Design Scheme

4.1. Design of the Rod Linkage Mechanism. During the design process two schemes were prepared for the rod linkage mechanism.

Scheme A is a parallelogram scheme, wherein the mechanism is fully linear and the movement of the electric motor's output arm can be completely reflected in the fuel control rod; the movement of the electric motor's arm and the fuel control rod is completely synchronized, with the force moments at the electric motor's arm and at the fuel control rod being equal. Scheme B is considered as an optimized scheme, promoting certain optimal force moment magnification characteristics for the mechanism and making the linearity of the mechanism across the whole slewing area as favorable as possible.

When the mechanism is in a parallelogramatic structure, the determination of the relevant parameters is relatively simple. The effective length of the output arm of the electric motor is equal to that of the fuel control rod, and their installation sites can be guaranteed to be parallel to each other. The length of link rod is determined according to the distance of the two ball pivots on said installation sites, and the included angles of the link rod with the output arm of the electric motor and with the fuel control rod should be as close to 90° as possible. Scheme B is more difficult than Scheme A in terms of design, as during the determination of the spatial structure, it is necessary to consider the electric motor's rotation angle, force moment magnification characteristics, and the mechanism's linear characteristics together with the spatial arrangement.

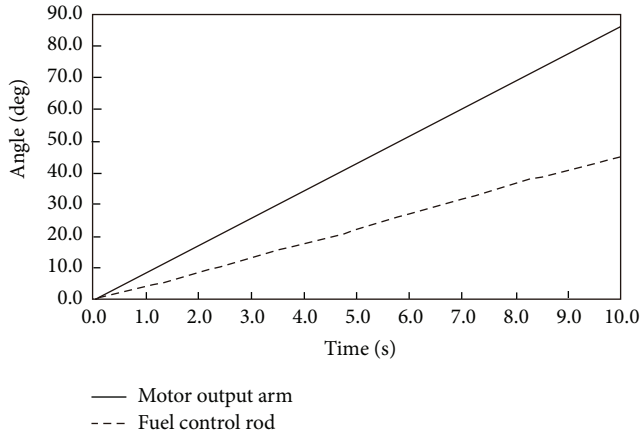

Figure 5: Relationship between the rotation angle of the electric motor's output arm and that of fuel control rod under Scheme B.

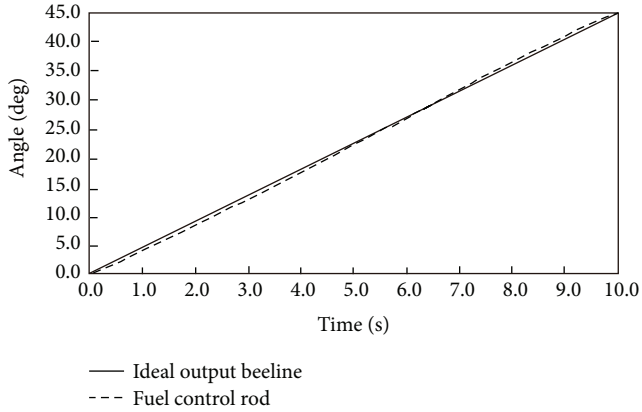

Figure 6: Comparison diagram of the output curve of the rotation angle of fuel control rod and the ideal output beeline under Scheme B.

Figure 5 shows the relationship between the rotation angle of the electric motor's output arm and the rotation angle of the fuel control rod under Scheme B.

Figure 5 indicates that although the mechanism in Scheme B is not in the shape of a parallelogram, the linearity is extremely high and the motion of the electric motor's output arm is reflected in the rotary shaft of the fuel control rod in almost geometric proportions.

Figure 6 is a diagram comparing the output curve of the rotation angle of the fuel control rod and the ideal output beeline under Scheme B.

Figure 6 shows that when Scheme B is adopted, the position linearity of the rotation angle of the fuel control rod is extremely high, which is quite favorable to developing the motor's control software.

Figure 7 displays the relationship between the angular velocity of the electric motor's output arm and that of the fuel control rod under Scheme B.

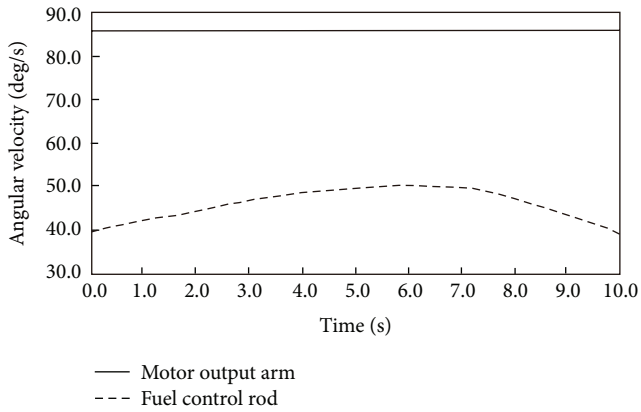

Figure 7: Relationship between the angular velocity of electric motor's output arm and that of the fuel control rod under Scheme B.

As indicated in Figure 7, the output force moment of the electric motor's output arm is magnified during its transfer to the fuel control rod. The magnification ratio of the drive mechanism at the minimal position of the fuel control rod is 2.13 and it is 2.25 while at the maximal position. The smallest magnification ratio is 1.80, when the angular velocity of the fuel control rod is at its maximal value, and the average magnification ratio of the system is 1.91.

According to the results of the simulation using Scheme B, there are almost no obvious differences from Scheme A in terms of position linearity, with both these two schemes having an ideal linear relationship. Regarding force moment magnification characteristics, the magnification ratio of the drive mechanism in Scheme B is close to 2 and relatively stable. Under Scheme B the electric motor has an 86° rotation angle, compared to 45° under Scheme A. So the scheme B is preferable in terms of control precision.

4.2. Structural Design and Strength Checking of the Drive Mechanism's Parts. The design of the drive mechanism covers parts including the electric motor's output arm, the double-end bolt on the link rod, the retracting spring, the stay bolt for connecting the fuel control rod, and the electric motor's mount support. Because of the comparatively less significant influence of the mechanism's weight and size characteristics, the processing performance of the parts is what should receive the most attention. The design should avoid complex structures as much as possible. Also, the strength checking is required to ensure that all parts meet their design requirements.

The load on the parts can be calculated according to the results measured for the fuel supply system's resisting moment and the restoring moment of the spring. Experiments revealed that the resisting moment, which is applied to the fuel control rod, is 3000 Nmm. The force on the mechanism over the whole working range can thus be solved by calculation of the obtained resisting moment. Figure 8 illustrates the curve of the loads on the electric motor's output arm under Scheme B.

The stress and deformation distribution of the electric motor's output arm can be obtained when the maximal value of the load curve of the engine's output arm in Figure 8, which is close to 250 N, is taken as the input force onto the screwed

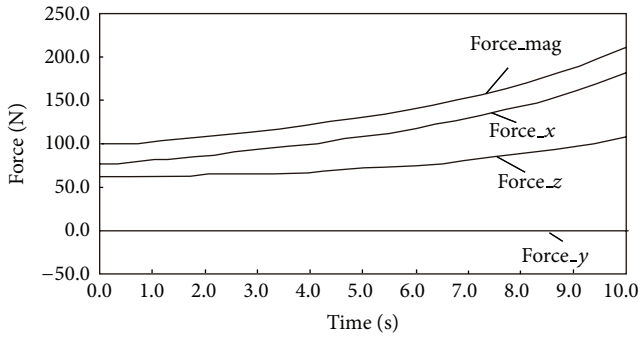

Figure 8: Load curve of electric motor's output arm under Scheme B.

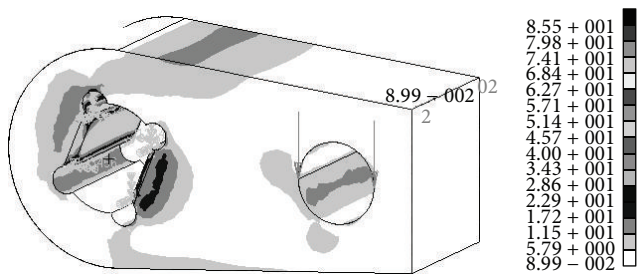

Figure 9: Stress distribution of electric motor's output arm under Scheme B.

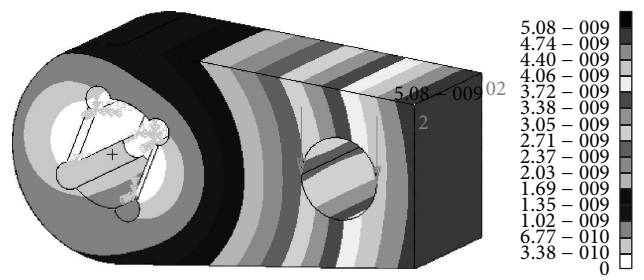

Figure 10: Deformation distribution of electric motor's output arm under Scheme B.

hole along the vertical direction. Figures 9 and 10 show the stress and deformation distributions of the electric motor's output arm under Scheme B, and they were created in Patran with a vertical force of 250 N and in a free tetrahedron grid.

Figures 9 and 10 reveal that the stress of the electric motor's output arm under Scheme B is significantly less than the yield limit of the material, and the electric motor's output arm can thus fully meet its strength requirements.

4.3. Assembly Design of the Drive Mechanism. Because the mechanism may swing back and forth during operation and the engine may vibrate, a locknut is required at each screw thread connection to ensure it remains locked in. Without a locknut or with a locknut insufficient in locking force, the screw thread connection may quickly loosen, causing clearance to occur in all parts of the mechanism and leading to a loss of control over the fuel control rod system. It is also necessary to apply a spring washer between the mount support and the engine housing, in order to prevent loosening. Installation of the electric motor requires the use of vibration isolation measures, so a rubber gasket is necessary between the electric motor and the mount support.

The sketch map of assembly under Scheme B is as shown in Figure 11.

5. Electronically Controlled Fuel Control Rod System Experiments

5.1. Introduction to the Experiment System. After analysis, design, processing, and assembly of the drive mechanism of the ECFCRS, bench tests and vehicle tests of the system were conducted. The sketch map of the bench test is given in Figure 12. The CPU of the electrically controlled unit (ECU) was MC68376, a 32-bit single chip microcontroller from Motorola, and the control program was written in the C language, with the software having been developed with the integrated development software WinIDEA. The desktop computer was connected with the ECU through a serial communications port so that it could monitor the working process of the ECFCRS. The same hardware and software as in the bench test were used in the real vehicle tests, except that a laptop computer was used instead of a desktop for communicating with the AMT ECU.

5.2. Bench Tests. The task of an ECFCRS is to follow the driver's operation of the accelerator pedal during the nongearshift period. The bench tests are conducted primarily for the purpose of verifying the engine speed following-up performance of the developed system.

Figure 13 describes the following-up process of the rotation angle of the fuel control rod along with the position signal of the accelerator pedal, where LTH refers to said fuel control rod rotation angle and LPD refers to the position signal of the accelerator pedal.

Figure 13 indicates that the developed system can not only follow the driver's operations of the accelerator pedal but also filter out high frequency vibrations, only responding to signals of lower frequency. The developed system thus has preferable engine speed following-up performance.

5.3. Vehicle Tests. Vehicle tests can be used to verify whether the developed ECFCRS has preferable engine speed following-up performance during nongearshift periods and preferable speed regulating performance during gear shifting up or down. Figure 14 contains the AMT vehicle test results when equipped with the developed ECFCRS, where N_E, N_1, and N_2 refer to engine speed, rotation speed of the transmission input shaft and rotation speed of the output shaft, respectively, TX and TY refer to the selective gear position signal and the gearing position signal, respectively, LC is the clutch displacement, PC is the pressure of the AMT hydraulic circuit, BK is the brake pedal position, and LTH and LPD are the rotation angle position signal of the fuel

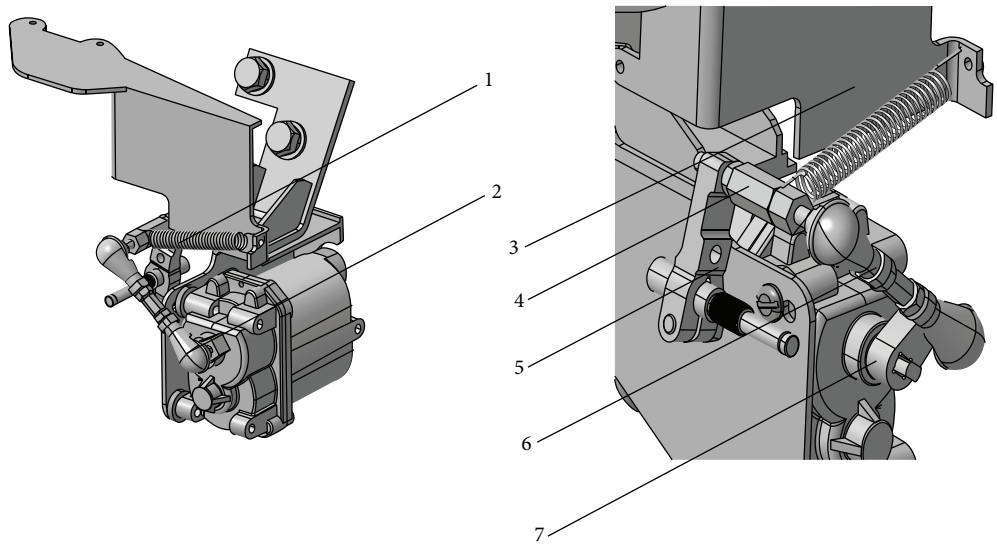

(1) Retracting spring
(2) Ball pivot
(3) Electric motor's bracket
(4) Push rod
(5) Fuel control rod
(6) Link rod
(7) Electric motor's output arm.

Figure 11: Sketch map of assembly under Scheme B.

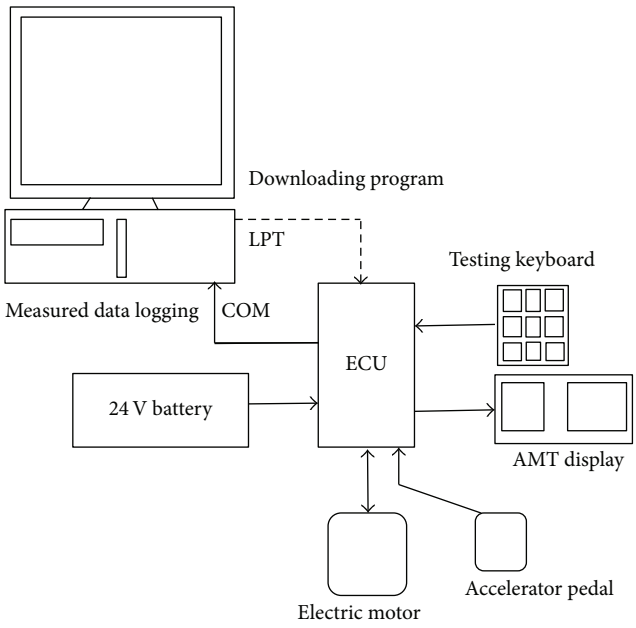

Figure 12: Sketch map of the bench test system.

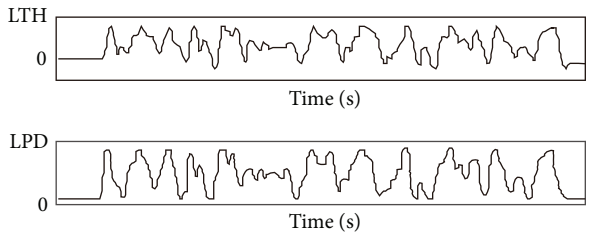

Figure 13: Following-up process of the rotation angle of the fuel control rod along with the position signal of the accelerator pedal.

control rod and the position signal of the accelerator pedal, respectively.

As shown in Figure 14, LTH can follow the movement of LPD during the nongearshift period; when the gears are shifting upwards, the electrically controlled fuel control rod system can automatically bring down the engine speed, taking the rotation speed of the transmission input shaft as its target value, while when the gears are shifting down, it can raise the engine speed, also targeting the rotation speed of the transmission input shaft. In this way, AMT with an electrically controlled fuel control rod system can not only produce significant ride comfort but also greatly shorten the synchronous time of driving and of the driven parts of the clutch, prolonging the clutch's lifespan.

6. Conclusions

Structural optimization principles and design for the drive mechanism of an ECFCRS for a diesel engine are proposed here, a new design method for the drive mechanism of the ECFCRS is developed, different design schemes are compared, the design philosophy of all parts of the drive mechanism is presented, the methods for structural design and strength checking of the parts are introduced, and the principles of the assembly design are discussed. The results of bench tests and vehicle tests are also discussed. These bench

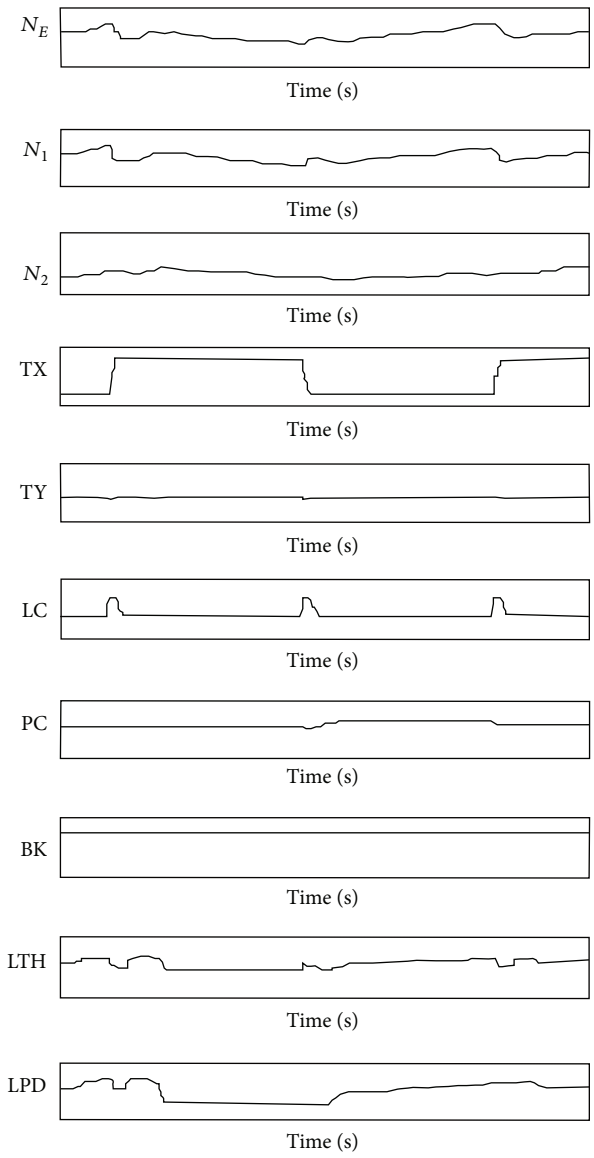

Figure 14: AMT vehicle test results equipped with the developed electronically controlled fuel control rod system.

tests and vehicle tests indicate that the developed ECFCRS has preferable engine speed following-up performance and engine speed regulating performance, with a significantly shortened design cycle. Thus, for an AMT vehicle, not only can the ride comfort be improved but the lifespan of the clutch can also be prolonged. The proposed design method also has significance as a reference for developing other vehicle systems.

Conflict of Interests

The authors declare that there is no conflict of interests regarding the publication of this paper.

Acknowledgment

This work was supported by the National Natural Science Foundation of China (Grant no. 51375053).

References

[1] G. Lucente, M. Montanari, and C. Rossi, "Modelling of an automated manual transmission system," *Mechatronics*, vol. 17, no. 2-3, pp. 73–91, 2007.

[2] Y. Lei, B. Gao, H. Tian, A. Ge, and S. Yan, "Throttle control strategies in the process of integrated powertrain control," *Chinese Journal of Mechanical Engineering*, vol. 18, no. 3, pp. 429–433, 2005.

[3] A. Turner, K. Ramsay, R. Clark, and D. Howe, "Direct-drive electromechanical linear actuator for shift-by-wire control of an automated transmission," in *Proceedings of the IEEE International Conference on Vehicle Power and Propulsion*, Windsor, Conn, USA, 2006.

[4] S. E. Moon, M. S. Kim, H. Yeo et al., "Design and implementation of clutch-by-wire system for automated manual transmissions," *International Journal of Vehicle Design*, vol. 36, no. 1, pp. 83–100, 2004.

[5] C. H. Tseng and M. F. Hsieh, "Analysis and optimization of clutch actuator on automated manual transmission system," SAE Technical Paper 2005-01-1782, SAE, Detroit, Mich, USA, 2005.

[6] H. Tanaka and H. Wada, "Fuzzy control of clutch engagement for automated manual transmission," *Vehicle System Dynamics*, vol. 24, no. 4-5, pp. 365–376, 1995.

[7] X.-Y. Song, Z.-X. Sun, X.-J. Yang, and G.-M. Zhu, "Modelling, control, and hardware-in-the-loop simulation of an automated manual transmission," *Proceedings of the Institution of Mechanical Engineers Part D: Journal of Automobile Engineering*, vol. 224, no. 2, pp. 143–160, 2010.

[8] E. Galvagno, M. Velardocchia, and A. Vigliani, "Analysis and simulation of a torque assist automated manual transmission," *Mechanical Systems & Signal Processing*, vol. 25, no. 6, pp. 1877–1886, 2011.

[9] Y.-S. Zhao, Z.-F. Liu, L.-G. Cai, W.-T. Yang, J. Yang, and Z. Luo, "Study of control for the automated clutch of an automated manual transmission vehicle based on rapid control prototyping," *Proceedings of the Institution of Mechanical Engineers, Part D: Journal of Automobile Engineering*, vol. 224, no. 4, pp. 475–487, 2010.

[10] L. Glielmo, L. Iannelli, V. Vacca, and F. Vasca, "Gearshift control for automated manual transmissions," *IEEE/ASME Transactions on Mechatronics*, vol. 11, no. 1, pp. 17–26, 2006.

[11] B. Mashadi and A. Kazemkhani, "A fuzzy gear shifting strategy for manual transmissions," in *Control Systems and Robotics (ICMIT '05)*, vol. 6042 of *Proceedings of SPIE, 60424M*, 2005.

[12] K. van Berkel, F. Veldpaus, T. Hofman, B. Vroemen, and M. Steinbuch, "Fast and smooth clutch engagement control for a mechanical hybrid powertrain," *IEEE Transactions on Control Systems Technology*, vol. 22, no. 4, pp. 1241–1254, 2014.

[13] P. D. Walker and N. Zhang, "Engagement and control of synchroniser mechanisms in dual clutch transmissions," *Mechanical Systems and Signal Processing*, vol. 26, no. 1, pp. 320–332, 2012.

[14] Y. Lei and H. Tian, "Research on accurate engagement control of electrohydraulic clutch actuator," SAE Technical Paper 2005-01-1787, SAE International, Detroit, Mich, USA, 2005.

[15] L. Glielmo, L. Iannelli, V. Vacca, and F. Vasca, "Speed control for automated manual transmission with dry clutch," in *Proceedings of the 43rd IEEE Conference on Decision and Control (CDC '04)*, vol. 2, pp. 1709–1714, Atlantis, Bahamas, December 2004.

[16] R. Loh, W. Thanom, J. Pyko, and A. Lee, "Electronic throttle control system: modeling, identification and model-based control designs," *Engineering*, vol. 5, no. 7, pp. 587–600, 2013.

[17] G. Panzani, M. Corno, and S. M. Savaresi, "On adaptive electronic throttle control for sport motorcycles," *Control Engineering Practice*, vol. 21, no. 1, pp. 42–53, 2013.

[18] A. Salem, B. Jens, and M. Nathan, "Tuning an electronic throttle controllers using computer-aided calibration methods," SAE Technical Paper 2006-01-0307, SAE, Detroit, Mich, USA, 2006.

[19] X. Yin, D. Xue, and Y. Cai, "Application of time-optimal strategy and fuzzy logic to the engine speed control during the gear-shifting process of AMT," in *Proceedings of the 4th International Conference on Fuzzy Systems and Knowledge Discovery (FSKD '07)*, vol. 4, pp. 468–472, August 2007.